PHYSICAL REVIEW B **92**, 161113(R) (2015)

Efficient formalism for warm dense matter simulations

Attila Cangi[1,*] and Aurora Pribram-Jones[2]
[1]*Max Planck Institute of Microstructure Physics, Weinberg 2, 06120 Halle (Saale), Germany*
[2]*Department of Chemistry, University of California, Irvine, California 92697-2025, USA*
(Received 27 October 2014; revised manuscript received 24 September 2015; published 16 October 2015)

Simulation of warm dense matter requires computational methods that capture both quantum and classical behavior efficiently under high-temperature, high-density conditions. Currently, density functional theory molecular dynamics is used to model electrons and ions, but this method's computational cost skyrockets as temperatures and densities increase. We propose finite-temperature potential functional theory as an in-principle-exact alternative that suffers no such drawback. We derive an orbital-free free energy approximation through a coupling-constant formalism. Our density approximation and its associated free energy approximation demonstrate the method's accuracy and efficiency.

DOI: 10.1103/PhysRevB.92.161113 PACS number(s): 52.65.−y, 31.15.E−, 71.15.Mb

Warm dense matter (WDM) is a highly energetic phase of matter with characteristics of both solids and plasmas [1]. The high temperatures and pressures necessary for creation of WDM are present in the centers of giant planets and on the path to ignition of inertial confinement fusion capsules [2,3]. The high cost of experiments in this region of phase space has led to renewed interest and great progress in its theoretical treatment [4–6]. Traditional plasma and condensed matter theoretical approaches exhibit serious shortcomings [1], leading to the WDM regime's characterization as the "malfunction junction." Since both quantum and classical effects are crucial to accurate WDM simulations [7], density functional theory (DFT) molecular dynamics has been used with increasing frequency [8]. This method relies on Kohn-Sham (KS) DFT, which simplifies solving the interacting problem of interest by mapping it onto a non-interacting system [9,10]. While the agreement between these calculations and experimental results is excellent [11,12], the calculations remain incredibly expensive [13,14]. The computational bottleneck in these calculations is the solution of the KS equations, a step that becomes increasingly expensive as temperatures and fractional occupations rise. In fact, the cost exhibits nearly exponential scaling with temperature due to the KS cycle including many states at WDM temperatures [15].

A solution to this problem is orbital-free DFT [16], which avoids this costly step using noninteracting kinetic energy approximations that depend directly on the electronic density. Because the kinetic energy is such a large fraction of the total energy, however, these approximations must be highly accurate to be of practical use. Though much progress has been made for WDM [17–19], approximations are complicated by temperature effects. The KS kentropy, the free energy consisting of the noninteracting kinetic energy and entropy, must be approximated directly, greatly complicating the production of useful, efficient approximations.

At zero temperature, potential functional theory (PFT) is a promising approach to the electronic structure problem [20,21]. It is also orbital-free, but skirts the troublesome issue of separately approximating the KS kinetic energy. PFT's coupling-constant formalism automatically generates a highly accurate kinetic energy potential functional approximation (PFA) for any density PFA [20]. In this way, one needs only find a sufficiently accurate density approximation [22]. Approximations to the noninteracting density have been derived in various semiclassical [22–24], and stochastic approaches [25]. Most closely related to this work is the pioneering path-integral formalism of Yang [26,27] which goes beyond the gradient expansion at finite temperature. An advantage of PFT is that it generates leading corrections to zero-temperature local approximations [22], which become exact in the well-known Lieb limit [28]. Finite-temperature Thomas-Fermi theory [29,30] becomes relatively exact for nonzero temperatures under similar scaling [31]. In this way, our method provides a pathway to systematic improvements to approximations, something generally missing from DFT approaches.

The particular scaling conditions under which TF becomes exact for all temperatures is related to the breakdown of purely quantum or classical behavior as both temperatures and particle numbers increase [1]. The importance of both these effects in the WDM regime underlies its theoretical complexity [32]. It is useful to represent the influences of temperature and density with a single electron degeneracy parameter defined by $\Lambda = \tau/\mu$, which depends on the system temperature τ and temperature-dependent chemical potential μ. Then, the WDM regime can be defined as where $\Lambda \approx 1$. At these conditions, KS-DFT is hugely expensive, while traditional plasma methods miss critical electronic structure features. In Fig. 1, density oscillations still present at WDM conditions are neglected by the smooth, classical TF approximation and its conventional gradient correction (GEA2) but are captured by our method.

In this Rapid Communication, we (i) derive PFT for thermal ensembles, (ii) give an explicit equation for the kentropy relying solely on the temperature-dependent density, (iii) derive and implement a highly accurate density approximation in one dimension to illustrate our general result, and (iv) perform (orbital-free) PFT calculations in the WDM regime. Our method generates highly accurate approximations, skirts the need for separate kentropy approximations, provides a road map for systematic improvement, and converges rapidly as temperatures increase while maintaining

*acangi@mpi-halle.mpg.de

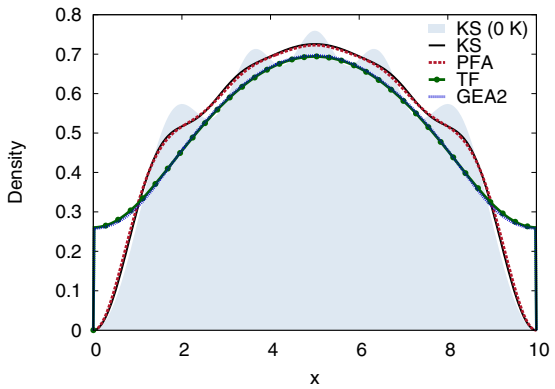

FIG. 1. (Color online) Shortcomings of the TF approximation in the WDM regime: Total density of five particles in the potential $v(x) = -2\sin^2(\pi x/10)$ within a box (of size 10 a.u.) at $\Lambda = \tau/\mu = 0.93$. Compare the exact density (solid black curve) with our PFA (dashed red curve) derived in Eq. (11), which is basically on top of the exact result. On the other hand, the TF approximation (dotted green curve) and conventional (second-order) gradient expansion (short-dashed blue, GEA2) capture the general qualitative features but completely miss the quantum oscillations. We also show the corresponding exact density at zero temperature (light blue shaded area), with its pronounced oscillations that smooth as temperatures rise.

accuracy at low temperatures. It also bridges low and high temperature methods and so is uniquely suited to WDM.

At nonzero temperature, the energy is replaced by the grand canonical potential as the quantity of interest. The grand canonical Hamiltonian is written

$$\hat{\Omega} = \hat{H} - \tau\hat{S} - \mu\hat{N}, \tag{1}$$

where $\hat{H}$, $\hat{S}$, and $\hat{N}$ are the Hamiltonian, entropy, and particle-number operators. In electronic structure theory, we typically deal with nonrelativistic electrons within the Born-Oppenheimer approximation. The electronic Hamiltonian (in atomic units here and thereafter) reads

$$\hat{H} = \hat{T} + \hat{V}_{\rm ee} + \hat{V}\,, \tag{2}$$

where $\hat{T}$ denotes the kinetic energy operator, $\hat{V}_{\rm ee}$ the interelectronic repulsion, and $v(\mathbf{r})$ the static external potential in which the electrons move. (We suppress spin for simplicity of notation.) In his seminal work [33], Mermin established thermal DFT. Eschrig defined a well-behaved domain for densities, showed the differentiability of the universal functional, and extended thermal DFT to include spin [34]. More recently, several exact conditions were derived [32,35].

Dual to thermal DFT, we write the grand canonical potential in terms of potential functionals (denoted by square brackets):

$$\Omega^{\tau}_{v-\mu} = F^{\tau}[v] + \int d^3r n^{\tau}[v](\mathbf{r})(v(\mathbf{r}) - \mu). \tag{3}$$

Here, $F^{\tau}[v]{=}F^{\tau}[\hat{\Gamma}^0_{v-\mu}]{=}T[\hat{\Gamma}^0_{v-\mu}]{+}V_{ee}[\hat{\Gamma}^0_{v-\mu}] - \tau S[\hat{\Gamma}^0_{v-\mu}]$ denotes the universal functional in terms of the equilibrium statistical operator $\hat{\Gamma}^0_{v-\mu}$, which captures all system-independent behavior in thermal DFT.

In practice, approximating this expression would require two separate approximate potential functionals, one for the universal finite-temperature functional and one for the density:

$$\breve{\Omega}^{\tau}_{v-\mu} = \breve{F}^{\tau}[v] + \int d^3r \breve{n}^{\tau}[v](\mathbf{r})(v(\mathbf{r}) - \mu). \tag{4}$$

However, we can generate an approximation (denoted by a breve above the approximated quantity) to the universal functional that corresponds to any chosen density approximation. In analogy to the zero-temperature case [20], we introduce a coupling constant λ in the one-body potential, $v^{\lambda}(\mathbf{r}) = (1-\lambda)v_0(\mathbf{r}) + \lambda v(\mathbf{r})$, where v_0 is some reference potential. Via the Hellmann-Feynman theorem, we rewrite the grand potential,

$$\Omega^{\tau}_{v-\mu} = \Omega^{\tau}_0 + \int_0^1 d\lambda \int d^3r n^{\tau}[v^{\lambda}](\mathbf{r})\Delta v(\mathbf{r}), \tag{5}$$

where $\Delta v(\mathbf{r}) = v(\mathbf{r}) - v_0(\mathbf{r})$ and Ω^{τ}_0 is the reference system grand potential. Setting $v_0 = 0$ and defining $\bar{n}^{\tau}[v](\mathbf{r}) = \int_0^1 d\lambda\, n^{\tau}[v^{\lambda}](\mathbf{r})$, we now write the exact finite-temperature universal functional in terms of the density written as a potential functional:

$$F^{\tau}[v] = \int d^3r\{\bar{n}^{\tau}[v](\mathbf{r}) - n^{\tau}[v](\mathbf{r})\}v(\mathbf{r}). \tag{6}$$

This defines an approximate functional $\breve{F}^{\tau}[v]$ corresponding to the chosen density approximation $\breve{n}^{\tau}$ and is the generalization of PFT to thermal ensembles. The coupling-constant approach differentiates the present formalism from previous ground breaking work in Refs. [27] and [36].

Practical use of this formula as written would require sufficiently accurate approximations to the interacting electron density. These are likely unavailable, so we instead apply it to the noninteracting electrons of the KS system. In DFT, the KS system is a clever way of approximating the exact F^{τ} by mapping the interacting system to a noninteracting system with the same electronic density and temperature. This determines the one-body KS potential and corresponding chemical potential. Through this mapping, the noninteracting, finite-temperature universal density functional is defined [35]

$$\tilde{F}^{\tau}_{\rm S}[n] := \min_{\hat{\Gamma}\to n} K^{\tau}[\hat{\Gamma}] = K^{\tau}\big[\hat{\Gamma}^{\tau}_{\rm s}[n]\big] = \tilde{K}^{\tau}_{\rm s}[n]\,. \tag{7}$$

The noninteracting kentropy $\tilde{K}_{\rm s}[n] = \tilde{T}_{\rm s}[n] - \tau\tilde{S}_{\rm s}[n]$ generates the KS equations and the KS orbitals, and tildes denote density functionals. The orbitals are implicit functionals of the density via the KS equations, and the average density is constructed by Fermi-weighted summing of the orbitals. Solution of these equations at every time step is the most costly step of DFT molecular dynamics.

The KS potential is defined [20,21]

$$v_{\rm S}(\mathbf{r}) = v(\mathbf{r}) + \tilde{v}_{\rm H}\big[n^{\tau}_{\rm S}[v_{\rm S}]\big](\mathbf{r}) + \tilde{v}_{\rm XC}\big[n^{\tau}_{\rm S}[v_{\rm S}]\big](\mathbf{r})\,, \tag{8}$$

where, in contrast to KS-DFT, the density is posed as a *potential* functional. All many-body interactions among the electrons are captured in the usual KS-DFT sense, via the (traditionally defined) Hartree and XC potentials [37]. The difference from a usual KS-DFT calculation is that Eq. (8) in conjunction with an approximation to the noninteracting density *bypasses* the hugely expensive iterative solution of the KS equations for WDM. Choosing a *potential* functional approximation to the noninteracting density automatically

generates an approximated KS potential, as illustrated in the Supplemental Material [38]. Once the self-consistent KS potential is determined, the KS kentropy is computed from

$$K_{\rm S}^{\tau}[v_{\rm S}] = \int d^3r \left\{\bar{n}_{\rm S}^{\tau}(\mathbf{r}) - n_{\rm S}^{\tau}[v_{\rm S}](\mathbf{r})\right\} v_{\rm S}(\mathbf{r}), \tag{9}$$

which is the analog of Eq. (6) for KS electrons. Again, Eq. (9) defines a coupling-constant approximation $\check{K}_{\rm S}^{\tau}[v_{\rm S}]$ when evaluated on any chosen approximation to the noninteracting density $\check{n}_{\rm S}^{\tau}$. Finally, the grand potential expressed in terms of KS quantities [35],

$$\Omega_{v-\mu}^{\tau} = K_{\rm S}^{\tau}[v_{\rm S}] + \tilde{U}\left[n_{\rm S}^{\tau}[v_{\rm S}]\right] + \tilde{\mathcal{F}}_{xc}^{\tau}\left[n_{\rm S}^{\tau}[v_{\rm S}]\right] + \int d^3r n^{\tau}[v_{\rm S}](\mathbf{r})(v(\mathbf{r}) - \mu), \tag{10}$$

can be evaluated via Eq. (9). Through this result, we leverage the body of time-proven XC approximations and eliminate the need to construct separate approximations to the KS kentropy for use in orbital-free (and thereby computationally inexpensive) schemes. Only an approximation to the noninteracting density is required. A general, systematic, nonempirical route to improved kentropy approximations is now available.

To illustrate the significance of our main result in Eq. (9), we consider a simple, yet useful, numerical demonstration: Noninteracting, spinless fermions in an arbitrary potential $v(x)$ confined to a box of size L obeying vanishing Dirichlet boundary conditions. (In a practical realization, this would be the self-consistent KS potential of the given many-body problem.) A starting point for deriving an approximation to the noninteracting density at finite temperature is the semiclassical propagator, which can be written as a convolution of the zero-temperature propagator with a factor carrying all temperature dependence [36]. From the propagator, we extract the density via an inverse Laplace transformation. Recently, a highly accurate PFA to the density was derived for this model using the path integral formalism and semiclassical techniques [39]. Here we extend this result to finite temperature and obtain:

$$\check{n}_{\rm S}^{\tau}(x) = \lim_{x'\to x} \sum_{\alpha=1}^{4} \sum_{j=0}^{\infty} \check{\gamma}_{\rm S}^{\tau}(x,x';\alpha,j)\,, \tag{11}$$

a PFA to the density at a given temperature and chemical potential, where

$$\check{\gamma}_{\rm S}^{\tau}(x,x';\alpha,j) = \frac{\tau \sin\Theta_{\mu}^{\alpha}(x,x';j)\,\mathrm{csch}\left[\pi\tau\mathcal{T}_{\mu}^{\alpha}(x,x';j)\right]}{(-1)^{\alpha+1}\sqrt{k_{\mu}(x)k_{\mu}(x')}}. \tag{12}$$

Here we define generalized classical phases $\Theta_{\mu}^{1}(x,x';j) = \theta_{\mu}^{-}(x,x') + 2j\theta_{\mu}(L)$, $\Theta_{\mu}^{2}(x,x';j) = \theta_{\mu}^{+}(x,x') + 2j\theta_{\mu}(L)$, $\Theta_{\mu}^{3}(x,x';j) = \theta_{\mu}^{-}(x,x') - 2(j+1)\theta_{\mu}(L)$, $\Theta_{\mu}^{4}(x,x';j) = \theta_{\mu}^{+}(x,x') - 2(j+1)\theta_{\mu}(L)$ and generalized classical traveling times $\mathcal{T}_{\mu}^{\alpha}(x,x';j) = d\Theta_{\mu}^{\alpha}(x,x';j)/d\mu$. Furthermore, $\theta^{\pm}(x,x') = \theta(x) \pm \theta(x')$, where $\theta_{\mu}(x) = \int_0^x dy\, k_{\mu}(y)$ and $k_{\mu}(x) = \sqrt{2(\mu - v(x))}$ at a given chemical potential μ, which is determined by normalization of the density.

The physical interpretation of our result in Eq. (11) is instructive: For a given chemical potential there are infinitely many classical paths that contribute to the total density. The paths are classified into four primitives (identified by α) onto which an integral number of periods (labelled by j) is added. The first primitive is special, in that it yields the TF density. However, higher-order terms in j do not yield the conventional gradient expansion. All other primitives and additional periods carry phase information about reflections from the boundaries, producing quantum density oscillations that greatly improve upon the TF result [39]. For more details, we refer to Ref. [39].

Our result in Eq. (11) can be evaluated numerically for a given temperature by truncating the infinite sum at an upper limit at which the sum has converged. Importantly for WDM applications, the higher the temperature, the lower the upper limit required for convergence of the sum. In fact, in the WDM regime only the leading term ($j = 1$) in the sum needs to be kept. Similar results have also been recently found at zero temperature [39,40], so this may be a universal feature due to the approximation's semiclassical nature.

However, the stationary phase approximation used to derive Eq. (11) yields the TF density at zero temperature as the leading term, i.e., $\lim_{x'\to x} \check{\gamma}_{\rm S}^{\tau}(x,x';1,0) = k_{\mu}(x)/\pi = \check{n}_{\rm TF}^{0}(x)$, instead of the finite-temperature TF density $\check{n}_{\rm TF}^{\tau}(x) = \sqrt{\tau/(2\pi)}\,F_{-1/2}(z)$, where $F_{\nu}(z) = \int_0^{\infty} da\, a^{\nu}[1 + \exp(a-z)]^{-1}$ and $z = k_{\mu}^2(x)/2\tau$. We fix this problem with an ad-hoc correction and ensure the correct boundary conditions. To do so, we replace the density from the first primitive $\lim_{x'\to x} \check{\gamma}_{\rm S}^{\tau}(x,x';1,0)$ with a Gaussian interpolation of $\check{n}_{\rm TF}^{0}(x)$ and $\check{n}_{\rm TF}^{\tau}(x)$. In this way, we cope with the density approaching the high-temperature limit (under which TF theory becomes exact) differently in two distinct regions, the interior of the box and the edge regions near the walls. These two distinct boundary layers have different asymptotic expansions in the high-temperature limit. The size of the edge-region boundary layers shrinks as the limit is approached. Our Gaussian interpolation is a crude version of the asymptotic matching used in boundary-layer theory [41].

In Fig. 1, we plot a typical density of five particles in the WDM regime ($\Lambda \approx 1$) in the potential $v(x) = -2\sin^2(\pi x/10)$ within a ten-unit box, along with approximate densities. The black curve is the exact result, the red dashed curve is our approximation, the green dotted curve is the TF density, and the short-dashed blue curve is the second-order gradient-corrected TF [36] density with the second-order gradient correction (GEA2) given by $-\partial_x^2 v(x)/\sqrt{512\pi\tau^3}F_{-5/2}(z) - 5(\partial_x v)^2/\sqrt{8192\pi\tau^5}F_{-7/2}(z)$. In addition, the light-blue shaded area denotes the corresponding density at zero temperature. Quantum oscillations in the density persist in the WDM regime, and TF theory completely fails to capture them. On the other hand, our PFA—derived to include quantum effects—is able to describe them properly and is therefore highly accurate. This mimics the results for cold densities seen in Fig. 1 of Ref. [22].

Next, we demonstrate the accuracy of our approach for kentropies. For our example, Eq. (9) simplifies to

$$\check{K}_{\rm S}^{\tau}[v] = K_{\rm S,0}^{\tau} + \int dx \left\{\check{n}_{\rm S}^{\tau}(x) - \check{n}_{\rm S}^{\tau}[v](x)\right\} v(x). \tag{13}$$

In this case the reference potential is not zero but an infinite square well. Hence, a kentropic contribution $K_{\rm S,0}^{\tau} = T_{\rm S,0}^{\tau} - \tau S_{\rm S,0}^{\tau}$ of the reference system appears, which we compute exactly. The kinetic energy of the infinite

TABLE I. Residual kentropy of five particles in the same potential as in Fig. 1. We list the error of the conventional TF approach, its gradient correction GEA2, and of our PFA [given in Eq. (13)] far below and above where WDM is typically encountered.

			Error × 10^2		
Λ	$K^\tau_{s,0}$	ΔK^τ_s	TF	GEA2	PFA
0.16	3.94	0.462	6.39	8.93	−0.32
0.31	3.87	0.461	7.16	9.85	−0.28
0.47	3.76	0.459	7.91	10.11	−0.31
0.62	3.64	0.456	8.39	10.01	−0.29
0.78	3.50	0.452	8.61	9.78	−0.30
0.93	3.34	0.448	8.65	9.52	−0.37
1.09	3.16	0.444	8.58	9.24	−0.50
1.40	2.77	0.435	8.21	8.63	−0.87
1.71	2.36	0.425	7.69	7.99	−1.27
2.02	1.92	0.414	7.13	7.35	−1.61
2.48	1.25	0.396	6.34	6.46	−1.86
2.94	0.58	0.378	5.64	5.69	−1.80
3.41	−0.10	0.360	5.04	5.04	−1.45
4.03	−0.99	0.338	4.37	4.33	−0.63

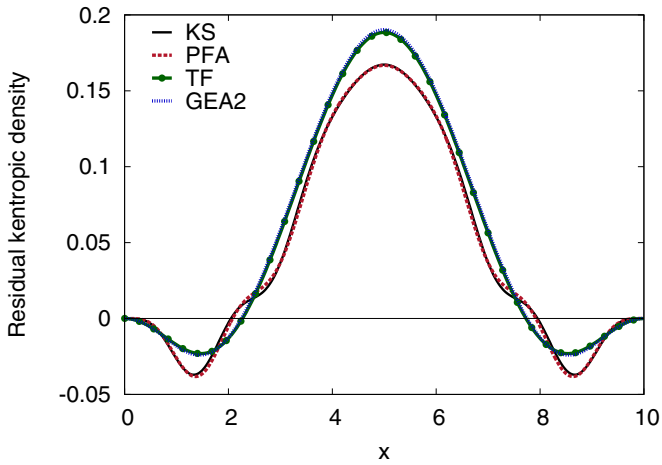

FIG. 2. (Color online) Residual kentropic density of five particles in the same potential as in Fig. 1 in the WDM regime. Our PFA (solid red curve) derived in Eq. (11) is on top of the exact result (solid black curve). TF (dotted green curve) and its gradient correction (short-dashed blue, GEA2), on the other hand, follow the general trend as expected but miss quantitative details.

square well is $T^\tau_{s,0} = \sum_j^N f^\tau_j \epsilon_{j,0}$, and the entropy is $S^\tau_{s,0} = -\sum_j f^\tau_j \ln(f^\tau_j) + (1 - f^\tau_j)\ln(1 - f^\tau_j)$, with $f^\tau_j = 1/(1.0 + \exp[(\epsilon_{j,0} - \mu_0)/\tau])$ denoting Fermi functions and $\epsilon_{j,0}$ and μ_0 the j^{th} eigenvalue and chemical potential. We avoid temperature-dependent KS eigenvalues [32] by choosing a purely noninteracting reference system, not a KS system associated with a specific interacting system. Evaluating Eq. (13) for the same potential as in Fig. 1 yields the results in Table I. We measure the error of TF theory, its gradient correction, and our PFA with respect to the residual kentropy $\Delta K^\tau_s = K^\tau_s - K^\tau_{s,0}$, because this is the only approximated piece of the kentropy. From cold temperatures up to the WDM regime ($\Lambda \approx 1$), our PFA yields kentropies that are significantly more accurate than either TF theory or the gradient expansion, improving them by roughly an order of magnitude. In fact, the gradient correction worsens the results, though it may improve them in other systems. In any case, the gradient correction is small, while our PFA yields dramatic improvements. Far beyond the WDM regime, the entropic contribution dominates, and the errors of all methods become comparable. In Table I, N is fixed as temperature increases. If instead N scales with increasing temperature, the system will approach a Lieb-like limit and TF accuracy is less than one percent for $\Lambda > 2$.

We can better understand the advantage of our PFA over the conventional TF approach by analyzing both in real space. We compute residual kentropic densities [the integrand of Eq. (13)] for the example in Fig. 1. As illustrated in Fig. 2, the TF approach (dotted green curve) and its gradient correction (short-dashed blue) only reproduce the qualitative trends of the exact result (black curve). Errors due to an overestimation in the interior are balanced by underestimation in the outer regions of the system. Our PFA, on the other hand, not only yields accurate integrated kentropies (area under the curve in Fig. 2), but is also highly accurate in real space. As such, and unlike TF, our PFA does not rely on cancellation of errors in the kentropy density for its accurate kentropy values.

The finite-temperature PFA approach outlined here offers several advantages over other methods, particularly for WDM, where solution of the KS equations for numerous occupied states becomes especially daunting. We retain the advantages of the KS system while avoiding the costly, repetitive solution of eigenvalue problems by isolating a piece of the kentropy to approximate through the coupling-constant formalism. Combined with our density approximation, this improves approximate kentropies by up to an order of magnitude in the WDM regime and produces highly accurate kentropic densities. This accuracy relies on inclusion of quantum oscillations beyond the minor corrections of the conventional gradient expansion. The density approximation derived in this paper is computationally efficient because only the leading term is needed for convergence at WDM temperatures.

The path integral method used to derive this approximation [39] invites use of successful zero-temperature approximations to the propagator, and it is a promising approach for extension to three dimensional systems. Furthermore, combining finite-temperature PFT with semiclassical methods offers prospects for a systematic route to exchange energy approximations, instead of relying on existing, zero-temperature density functional approximations. Work in this direction is currently in development. With these advantages, finite-temperature PFT is poised to bridge the "malfunction junction" of WDM by providing computationally efficient, semiclassical methods at high temperatures and densities.

We acknowledge Hardy Gross and Kieron Burke for providing an atmosphere facilitating independent research. We are grateful to Rudy Magyar for useful discussion. A.C. has been partially supported by NSF Grant No. CHE-1112442. A.P.J. is supported by DOE Grant No. DE-FG02-97ER25308.

[1] *Frontiers and Challenges in Warm Dense Matter*, Lecture Notes in Computational Science and Engineering, Vol. 96, edited by F. Graziani, M. P. Desjarlais, R. Redmer, and S. B. Trickey (Springer International Publishing, Heidelberg, 2014).

[2] S. Atzeni and J. Meyer-ter Vehn, *The Physics of Inertial Fusion: Beam-Plasma Interaction, Hydrodynamics, Hot Dense Matter* (Clarendon Press, Oxford, 2004).

[3] N. R. C. C. on High Energy Density Plasma Physics Plasma Science Committee, *Frontiers in High Energy Density Physics: The X-Games of Contemporary Science* (The National Academies Press, Washington, D.C., 2003).

[4] T. R. Mattsson and M. P. Desjarlais, Phys. Rev. Lett. **97**, 017801 (2006).

[5] F. R. Graziani, V. S. Batista, L. X. Benedict, J. I. Castor, H. Chen, S. N. Chen, C. A. Fichtl, J. N. Glosli, P. E. Grabowski, A. T. Graf, S. P. Hau-Riege, A. U. Hazi, S. A. Khairallah, L. Krauss, A. B. Langdon, R. A. London, A. Markmann, M. S. Murillo, D. F. Richards, H. A. Scott, R. Shepherd, L. G. Stanton, F. H. Streitz, M. P. Surh, J. C. Weisheit, and H. D. Whitley, High Energy Density Phys. **8**, 105 (2012).

[6] K. Y. Sanbonmatsu, L. E. Thode, H. X. Vu, and M. S. Murillo, J. Phys. IV (France) **10**, Pr5-259 (2000).

[7] M. D. Knudson and M. P. Desjarlais, Phys. Rev. Lett. **103**, 225501 (2009).

[8] B. Holst, R. Redmer, and M. P. Desjarlais, Phys. Rev. B **77**, 184201 (2008).

[9] P. Hohenberg and W. Kohn, Phys. Rev. **136**, B864 (1964).

[10] W. Kohn and L. J. Sham, Phys. Rev. **140**, A1133 (1965).

[11] A. Kietzmann, R. Redmer, M. P. Desjarlais, and T. R. Mattsson, Phys. Rev. Lett. **101**, 070401 (2008).

[12] S. Root, R. J. Magyar, J. H. Carpenter, D. L. Hanson, and T. R. Mattsson, Phys. Rev. Lett. **105**, 085501 (2010).

[13] D. Marx and J. Hutter, in *Modern Methods and Algorithms of Quantum Chemistry*, NIC Series, Vol. 1, edited by J. Grotendorst (Forschungszentrum, Jülich, Germany, 2000), pp. 301–449.

[14] D. Marx and J. Hutter, *Ab Initio Molecular Dynamics: Basic Theory and Advanced Methods* (Cambridge University Press, Cambridge, 2009).

[15] V. V. Karasiev, T. Sjostrom, D. Chakraborty, J. W. Dufty, K. Runge, F. E. Harris, and S. Trickey, in *Frontiers and Challenges in Warm Dense Matter*, Lecture Notes in Computational Science and Engineering, Vol. 96, edited by F. Graziani, M. P. Desjarlais, R. Redmer, and S. B. Trickey (Springer International Publishing, Heidelberg, 2014), pp. 61–85.

[16] Y. A. Wang and E. A. Carter, in *Theoretical Methods in Condensed Phase Chemistry*, edited by S. D. Schwartz (Kluwer, Dordrecht, 2000), Chap. 5, p. 117.

[17] V. V. Karasiev, T. Sjostrom, and S. B. Trickey, Phys. Rev. B **86**, 115101 (2012).

[18] V. V. Karasiev, D. Chakraborty, O. A. Shukruto, and S. B. Trickey, Phys. Rev. B **88**, 161108 (2013).

[19] T. Sjostrom and J. Daligault, Phys. Rev. B **88**, 195103 (2013).

[20] A. Cangi, D. Lee, P. Elliott, K. Burke, and E. K. U. Gross, Phys. Rev. Lett. **106**, 236404 (2011).

[21] A. Cangi, E. K. U. Gross, and K. Burke, Phys. Rev. A **88**, 062505 (2013).

[22] A. Cangi, D. Lee, P. Elliott, and K. Burke, Phys. Rev. B **81**, 235128 (2010).

[23] P. Elliott, D. Lee, A. Cangi, and K. Burke, Phys. Rev. Lett. **100**, 256406 (2008).

[24] J. Roccia, M. Brack, and A. Koch, Phys. Rev. E **81**, 011118 (2010).

[25] R. Baer, D. Neuhauser, and E. Rabani, Phys. Rev. Lett. **111**, 106402 (2013).

[26] W. Yang, Phys. Rev. A **38**, 5494 (1988).

[27] W. Yang, Phys. Rev. A **38**, 5504 (1988).

[28] E. Lieb and B. Simon, Phys. Rev. Lett. **31**, 681 (1973).

[29] L. Thomas, Math. Proc. Camb. Phil. Soc. **23**, 542 (1927).

[30] E. Fermi, Z. Phys. A **48**, 73 (1928).

[31] H. Narnhofer and W. Thirring, Ann. Phys. **134**, 128 (1981).

[32] A. Pribram-Jones, S. Pittalis, E. Gross, and K. Burke, in *Frontiers and Challenges in Warm Dense Matter*, Lecture Notes in Computational Science and Engineering, Vol. 96, edited by F. Graziani, M. P. Desjarlais, R. Redmer, and S. B. Trickey (Springer International Publishing, Heidelberg, 2014), pp. 25–60.

[33] N. D. Mermin, Phys. Rev. **137**, A1441 (1965).

[34] H. Eschrig, Phys. Rev. B **82**, 205120 (2010).

[35] S. Pittalis, C. R. Proetto, A. Floris, A. Sanna, C. Bersier, K. Burke, and E. K. U. Gross, Phys. Rev. Lett. **107**, 163001 (2011).

[36] J. Bartel, M. Brack, and M. Durand, Nucl. Phys. A **445**, 263 (1985).

[37] R. Dreizler and E. Gross, *Density Functional Theory: An Approach to the Quantum Many-Body Problem* (Springer-Verlag, Heidelberg, 1990).

[38] See Supplemental Material at http://link.aps.org/supplemental/10.1103/PhysRevB.92.161113 for self-consistent cycle of potential functional theory in the warm dense matter context.

[39] A. Cangi, E. Sim, and K. Burke (unpublished).

[40] J. Roccia and M. Brack, Phys. Rev. Lett. **100**, 200408 (2008).

[41] M. H. Holmes, *Introduction to Perturbation Methods* (Springer, New York, 2013).